ADVANCED ENERGY MATERIALS
www.advenergymat.de

High Performance Thermoelectricity in Earth-Abundant Compounds Based on Natural Mineral Tetrahedrites

Xu Lu, Donald T. Morelli, Yi Xia, Fei Zhou, Vidvuds Ozolins, Hang Chi, Xiaoyuan Zhou, and Ctirad Uher*

Thermoelectric materials can convert waste heat into electricity, potentially improving the efficiency of energy usage in both industry and everyday life. Unfortunately, known good thermoelectric materials often are comprised of elements that are in low abundance and require careful doping and complex synthesis procedures. Here, we report dimensionless thermoelectric figure of merit near unity in compounds of the form $Cu_{12-x}M_xSb_4S_{13}$, where *M* is a transition metal such as Zn or Fe, for wide ranges of *x*. The compounds investigated here span the range of compositions of the natural mineral family of tetrahedrites, the most widespread sulfosalts on Earth, and we further show that the natural mineral itself can be used directly as an inexpensive source thermoelectric material. Thermoelectrics comprised of earth-abundant elements will pave the way to many new, low cost thermoelectric energy generation opportunities.

1. Introduction

In the past few decades, thermoelectric materials have been a focus topic in solid-state physics and materials science due to their potential application in waste energy harvesting or Peltier cooling. The efficiency of thermoelectric materials is evaluated by the figure of merit ($zT = S^2\sigma T/\kappa$), where S is the Seebeck coefficient, σ the electrical conductivity, T the absolute temperature, and κ thermal conductivity. For many years, the benchmark for a good thermoelectric material has been zT of order unity, typified by Bi_2Te_3 and its alloys, which are used commercially in thermoelectric cooling modules. Over the last 15 years, with a more complete understanding of electronic and thermal transport in semiconductors, better control over synthesis methods, and the successful application of nanotechnology, new materials systems with zT values higher than unity have been discovered and developed, including thin film superlattices,[1] filled skutterudites,[2–6] and bulk nanostructured chalcogenides.[7–9] Unfortunately, many of these new materials are not suitable for large-scale application because of complex and costly synthesis procedures or the use of rare or toxic elements. A current challenge is the discovery of new thermoelectric materials which are inexpensive, environment-friendly, easy to synthesize, and comprised of earth-abundant elements. An interesting approach to this problem was recently described by Mehta et al.[10] who used a scalable, microwave-assisted method to produce bulk nanostructured bismuth telluride compounds.

One very successful route to improving zT in bulk solids is reduction of lattice thermal conductivity. For instance, the paradigm of "phonon glass/electron crystal (PGEC)" was introduced to describe materials which exhibit lattice thermal conductivity like a glassy or amorphous solid, and electronic properties of a good crystal.[11] For amorphous or glassy solids, the phonon mean free path approaches one interatomic spacing; the concept of a phonon mean free path shorter than one interatomic spacing loses its meaning, and thus this type of thermal transport has been termed "minimal" thermal conductivity.[12,13] Unfortunately, poor electrical conductivity in such amorphous solids prevents them from exhibiting high values of figure of merit. More interesting from the thermoelectric point of view are crystalline solids which exhibit very low thermal conductivity, due to strong intrinsic phonon scattering. Examples here include, in addition to the afore-mentioned skutterudites, complex cage structures such as clathrates.[14] Recently, exceptionally low thermal conductivity was discovered in crystalline rocksalt structure I-V-VI_2 compounds (e.g., $AgSbTe_2$), semiconductors typified by the lattice thermal conductivity of a glassy

X. Lu, Prof. D. T. Morelli
Department of Physics & Astronomy
Michigan State University
567 Wilson Road, East Lansing, Michigan 48824 USA
E-mail: dmorelli@egr.msu.edu
Prof. D. T. Morelli
Department of Chemical Engineering & Materials Science
Michigan State University
428 South Shaw Lane
East Lansing, Michigan 48824 USA
Y. Xia, Dr. F. Zhou, Prof. V. Ozolins
Department of Materials Science & Engineering
University of California, Los Angeles
410 Westwood Plaza, Los Angeles, California 90095 USA
H. Chi, Dr. X. Zhou, Prof. C. Uher
Department of Physics
450 Church Street
University of Michigan
Ann Arbor, Michigan 48109 USA

DOI: 10.1002/aenm.201200650

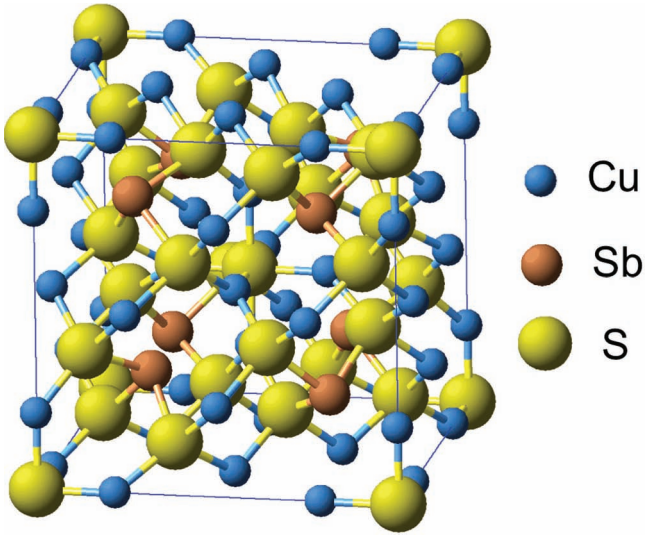

Figure 1. Crystal structure of tetrahedrite $Cu_{12}Sb_4S_{13}$. It contains two types of copper atoms: the first type is tetrahedrally coordinated to three sulfurs and one antimony, while the second exhibits three-fold planar coordination with three sulfurs. Twelve of the 13 sulfur atoms in the formula unit are tetrahedrally coordinated, while the sulfur at the corners and in the center of the cube has six Cu neighbors.

or amorphous system.[15] These materials exhibit electronic properties characteristic of good crystals and thus have demonstrated good thermoelectric behavior. Skoug and Morelli[16] identified a correlation between minimal thermal conductivity and the existence of an Sb lone s^2 pair in Sb-containing ternary semiconductors. Lone pair electrons induce strong lattice anharmonicity, the origin of lattice thermal resistance in solids.[17] Using density-functional theory (DFT) calculations, Zhang et al.[18] demonstrated explicitly the occurrence of large Grüneisen parameter in Cu_3SbSe_3 compounds and, using these parameters to calculate phonon scattering rates, were able to quantitatively account for the thermal conductivity using the Debye-Callaway formalism.[19]

$Cu_{12}Sb_4S_{13}$, the base composition of a large family of natural minerals called tetrahedrites, bears structural resemblance to the Cu_3SbSe_3 phase. It possesses a cubic sphalerite-like structure of $I\bar{4}3m$ symmetry[20] with six of the twelve Cu atoms occupying trigonal planar 12e sites and the remaining Cu atoms distributed on tetrahedral 12d sites (**Figure 1**). The Sb atoms also occupy a tetrahedral site but are bonded to only three sulfur atoms, leading to a void in the structure and a lone pair of electrons, just as in Cu_3SbSe_3. In terms of a simple crystal-chemical formula, four of the six tetrahedral sites are thought to be occupied by monovalent Cu, while the other two are occupied by Cu^{2+} ions; the trigonal planar sites are occupied solely by monovalent Cu.[21]

In this article we highlight the potential of directly using natural tetrahedrite minerals as high-temperature thermoelectric materials, without the need for time and energy consuming synthetic procedures or precise doping. We find that pure synthetic $Cu_{12}Sb_4S_{13}$ exhibits a zT value of 0.56 at 673 K (400 °C). This pure 12-4-13 composition does not occur in natural minerals. Rather, natural "tetrahedrite" is of typical composition $Cu_{12-x}M_x(Sb,As)_4S_{13}$, a solid solution of tetrahedrite ($Cu_{12}Sb_4S_{13}$) and tennantite ($Cu_{12}As_4S_{13}$) end-member compounds, with metal substitutions on the copper site. Whether a particular mineral is geologically termed tetrahedrite or tennantite is a somewhat arbitrary designation depending on where along this solid solution the particular mineral may lie. The tetrahedrite/tennantite mineral family is the most widespread sulfosalt on Earth, found quite typically with M = Zn, Fe, Hg and Mn. The most common substitution elements are Zn and Fe on Cu sites, up to $x = 2$ in the natural mineral.[22] Tetrahedrite ores are a main source of copper and one of the most important sources of silver worldwide. We report zT values of up to 0.95 near 700 K in synthetic $Cu_{12-x}(Zn,Fe)_xSb_4S_{13}$ with x = 0 to 1.5 and x = 0 to 0.7 for Zn and Fe, respectively. We further show that a comparable zT value can be obtained on a pellet processed *directly* from a natural mineral tetrahedrite specimen with a simple and quick adjustment of its composition. Our work opens a new route to discover and develop good thermoelectric materials from environmentally benign and earth abundant natural minerals.

2. Results and Discussion

Pure $Cu_{12}Sb_4S_{13}$ and compounds with substitution of Fe and Zn on the Cu site were synthesized using a standard vacuum, annealing, and hot-pressing procedure. The resulting samples are homogeneous, single phase and ≥98% theoretical density. We have observed no evidence of decomposition, either in the form of evaporation of sulfur or oxidation, up to the highest temperatures investigated in this study (720 K). **Figure 2**a shows the electrical resistivity of $Cu_{12-x}Zn_xSb_4S_{13}$ in the temperature range 373–673 K with x ranging from 0 to 1.5. The low temperature resistivity (not shown here) shows semiconductor-like characteristics but it cannot be fit with a simple activated behavior; rather, the conductivity behavior is more consistent with a hopping-type mechanism. In fact, our attempts to measure hole concentration using the Hall effect were unsuccessful; even in a field of several Tesla we find a Hall coefficient R_H close to zero. In terms of the crystal-chemical argument given above, this would imply that at least some of the nominally divalent Cu ions are in a monovalent or mixed valent state, giving rise to a partially filled Brillouin zone and metallic behavior. Indeed, DFT band structure calculations (Figure 2b) show that $Cu_{12}Sb_4S_{13}$ is a metal where the Fermi level falls near a sharp peak in the density-of-states (DOS) at the top of the valence band, and a semiconducting gap separates the valence bands from the conduction bands. The valence bands are formed by hybridizing sulfur 3p and copper 3d orbitals; the resulting complex has two unoccupied states per formula unit. Contrary to the naive valence counting argument given above, all copper ions are found to be in the monovalent Cu^+ state. We have verified that these conclusions remain qualitatively unchanged irrespective of the employed exchange-correlation functional. In pure and lightly Zn-substituted samples (x = 0, 0.5 and 1), resistivities are on the order of 10^{-5} ohm m, comparable to other good thermoelectric materials. When the Zn content is increased to $x = 1.5$, the resistivity increases by one order compared to the pure sample, and we find that for a Zn-substituted sample with $x = 2.0$ the sample is electrically insulating.

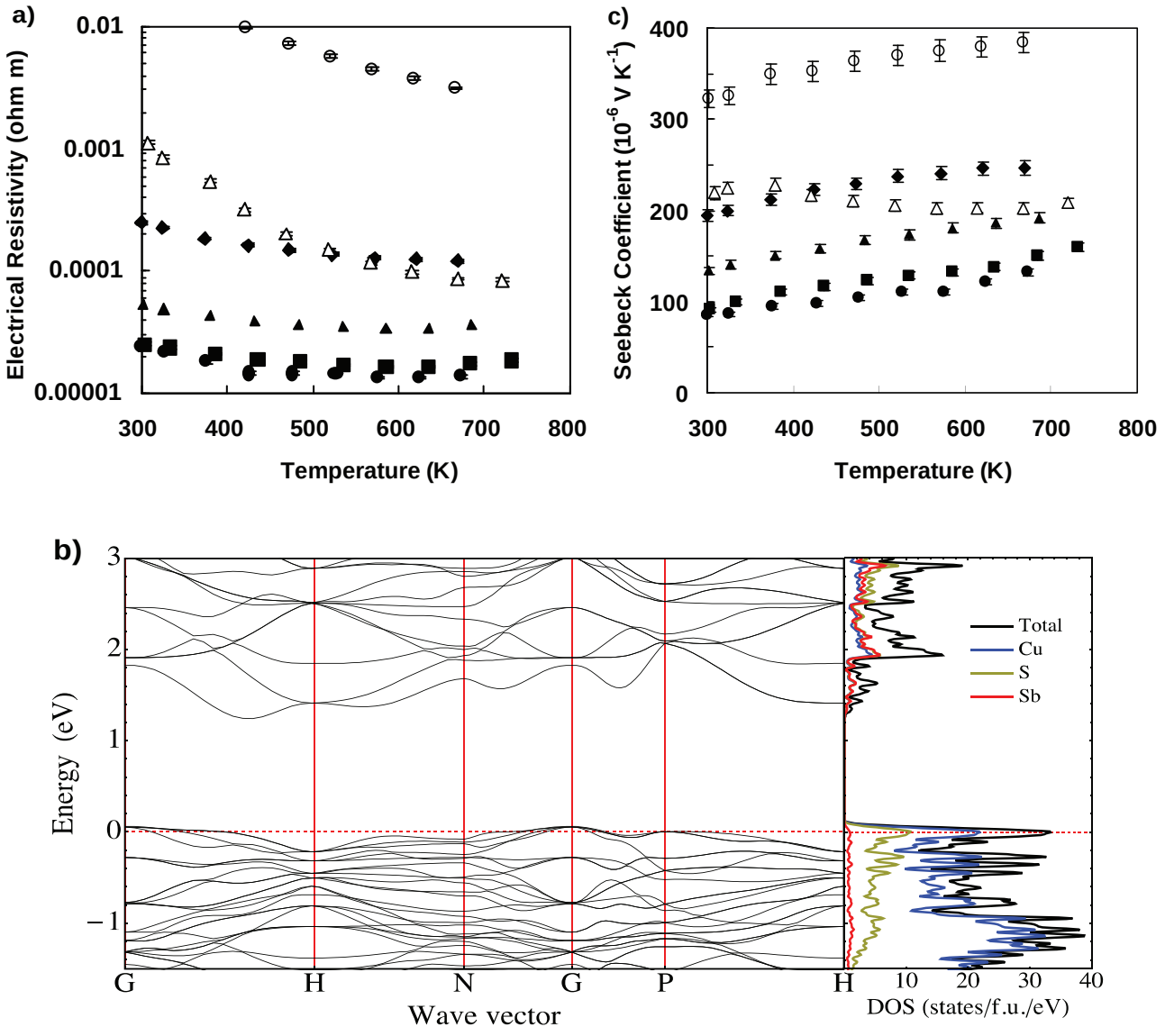

Figure 2. Electronic properties of tetrahedrite. a). electrical resistivity of powder-processed synthetic tetrahedrite pellets (closed symbols) of composition $Cu_{12-x}Zn_xSb_4S_{13}$ above room temperature (circles: x = 0; squares: x = 0.5; triangles: x = 1.0; diamonds: x = 1.5). The magnitude of the resistivity is in the range typical of good thermoelectric materials. For higher Zn substitution, holes in the valence band are filled and the material becomes insulating for x = 2. Open circles represent a pellet synthesized from natural tetrahedrite of nominal composition $Cu_{10.5}Fe_{1.5}As_{3.6}Sb_{0.4}S_{13}$, while the open triangles are for a pellet synthesized using a combination of this natural material and synthetic $Cu_{12}Sb_4S_{13}$. b). Electronic band structure and density-of states (DOS) of $Cu_{12}Sb_4S_{13}$. Fermi level is marked by a dashed line. Decomposition of the total DOS into contributions from Cu, Sb, and S shows the predominantly Cu 3d and S 3p character of valence bands. c). Seebeck coefficient of tetrahedrite of composition $Cu_{12-x}Zn_xSb_4S_{13}$; sample designation as in a). Seebeck coefficient rises strongly with temperature and Zn content, reaching values in excess of 200 μV K^{-1}. Like the resistivity, the Seebeck coefficient of the pellet synthesized using natural mineral tetrahedrite can be controlled by dilution with synthetic source material.

Since it is expected that the Zn ion will be strictly in the Zn^{2+} state, this is consistent with complete filling of the valence bands and the occurrence of a true semiconducting state. Our DFT calculations for $Cu_{10}Zn_2Sb_4S_{13}$ confirm this conclusion (see Supporting Information). These results are in contrast to those of Suekuni et al.[23] who measured a resistivity of ~10^{-3} ohm m at 300 K for $Cu_{10}Zn_2Sb_4S_{13}$; however the samples investigated in that study were only 75–80% dense and contained a secondary phase of Cu_3SbS_4.

As the Zn concentration is increased the Seebeck coefficient (Figure 2c) rises considerably, exceeding 200 μV K^{-1} at the highest temperatures for the $x = 1.5$ sample. This is consistent with the filling of holes in the valence band and pushing the Fermi level towards the steep slope of the DOS peak (Figure 2b) as zinc replaces copper. Above room temperature, with resistivity values in the 10^{-5} ohm m range and Seebeck coefficients ~100–200 μV K^{-1}, these tetrahedrites have thermoelectric power factors, $S^2\sigma$, comparable to some of the best thermoelectric materials (such as PbTe) in this temperature range.

Turning now to the thermal conductivity, **Figure 3**a displays thermal conductivity derived from our thermal diffusivity measurements above room temperature. We see that the thermal

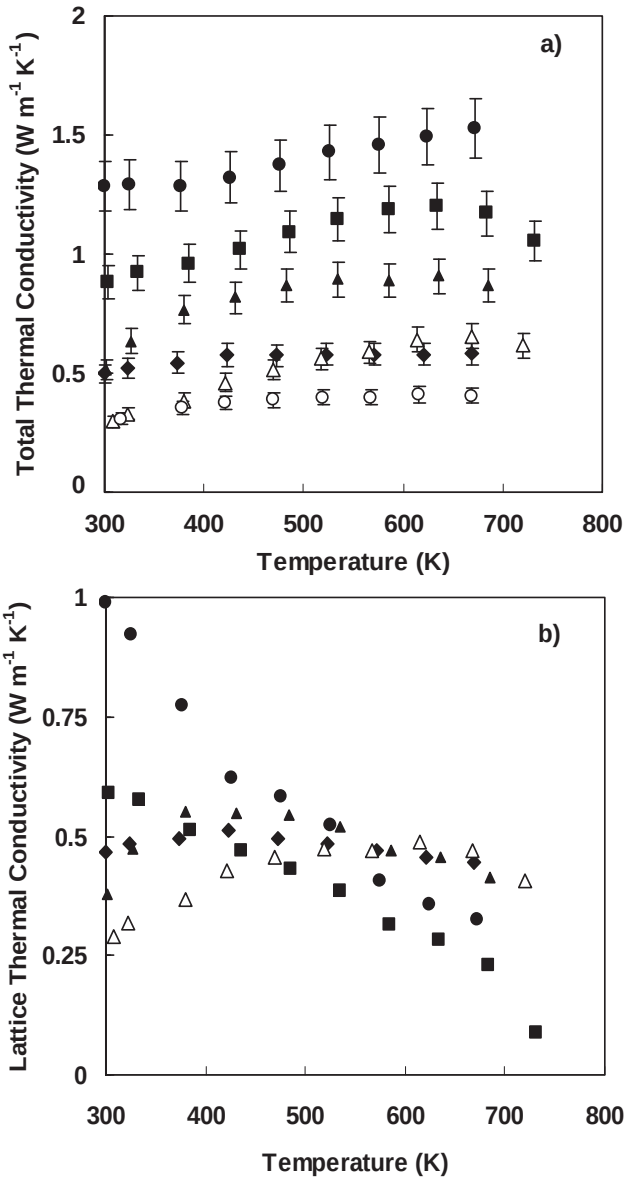

Figure 3. Thermal conductivity of tetrahedrite specimens. a) total and b) lattice thermal conductivities of $Cu_{12-x}Zn_xSb_4S_{13}$. The magnitude of the conductivity is comparable to or even smaller than typical thermoelectric materials like lead telluride or skutterudite. Zn-containing samples approach minimal thermal conductivity values over most of the temperature range, as does pure $Cu_{12}Sb_4S_{13}$ at the highest measurement temperatures.

conductivity is below 1.5 W m^{-1} K^{-1} over the entire temperature range. The thermal conductivity falls monotonically with increasing Zn substitution. This reflects the combined effects of a reduced electronic component of thermal conductivity and a decreasing lattice contribution. As an approximation, if we apply the Wiedemann-Franz law with Lorenz constant equal to its free-electron value to estimate the electronic contribution, we can extract the lattice thermal conductivity of our samples; the result is shown in Figure 3b. We see that while the pure sample still has a decreasing lattice thermal conductivity with increasing temperature, the Zn-substituted samples all have lattice thermal conductivity <0.5 W m^{-1} K^{-1}, and, in fact, even the pure tetrahedrite sample falls into this range at the highest temperature. This value of lattice thermal conductivity is close to the "minimal" thermal conductivity for a phonon mean free path equal to the interatomic spacing.

In order to help understand the low thermal conductivity in tetrahedrites, we have performed phonon dispersion calculations using the DFT linear response method, including calculations of the mode Grüneisen parameters. A prominent feature of the phonon dispersion (**Figure 4**) is the appearance of three harmonically unstable optical phonon branches involving out-of-plane vibrations of the three-fold coordinated Cu ions. Furthermore, transverse acoustic (TA) branches also become harmonically unstable near the zone-boundary N and P points. The depth of the minima in the potential energy surface obtained by following the unstable mode eigenvectors are a few tens of meV per formula unit (see Supporting Information). We hypothesize that structural disorder due to random freezing-in of the unstable phonons is a major reason for the variable-range hopping type conduction observed in this material at low temperatures. We also find that the frequencies of the TA branches are highly sensitive to volume changes resulting in calculated Grüneisen parameters above 10 (see Supporting Information). Since the intrinsic phonon scattering rates are proportional to the square of the Grüneisen parameter, this highly anharmonic behavior will produce strong intrinsic phonon scattering and large thermal resistance in these compounds.

The combination of high thermoelectric power factor and low thermal conductivity in these compounds leads to large thermoelectric figure of merit (**Figure 5**a). Although the power factor of the $x = 1.5$ sample is less than half that of the $x = 0$ sample, the zT value at $x = 1.5$ is still higher than that of pure sample, approaching 0.7 at 673 K. The maximum zT value near unity is attained for $x = 1$ at 720 K. The high zT values are maintained for relatively large Zn substitutions due to the compensating effect from the reduction in thermal conductivity. As can be seen from Figure 5a, the total thermal conductivity of the $x = 1.5$ sample was reduced to one third of that of pure sample at high temperature. The reduction in total thermal conductivity can be mainly attributed to the decreased electronic thermal conductivity. Because the lattice thermal conductivity in these compounds is so low, we find, somewhat ironically, that reducing the power factor actually leads to a 60% *enhancement* in zT value for the case of the $x = 1$ for Zn substitution, due to reduction in electronic thermal conductivity.

We have also measured the thermoelectric properties of synthetic $Cu_{12-x}Fe_xSb_4S_{13}$ ($x = 0.2$, 0.5, and 0.7). Like their Zn substituted counterparts, the Fe substituted samples display similar trends of an increase in resistivity, enhancement in the Seebeck coefficient and reduction in the total thermal conductivity. The zT value reaches a maximum of over 0.8 at $x = 0.5$ and decreases for higher values of x. Interestingly, the resistivity of $Cu_{11}FeSb_4S_{13}$ is three orders of magnitude larger than that of $Cu_{11}ZnSb_4S_{13}$. This difference between Fe and Zn substitution has its origin in the different valence states of Fe and Zn in tetrahedrite. Makovicky et al.[24] have shown that Fe in synthetic $Cu_{12-x}Fe_xSb_4S_{13}$ is trivalent for $0 < x < 1$ and divalent for $1 \leq x \leq 2$. This implies that, in the composition range measured

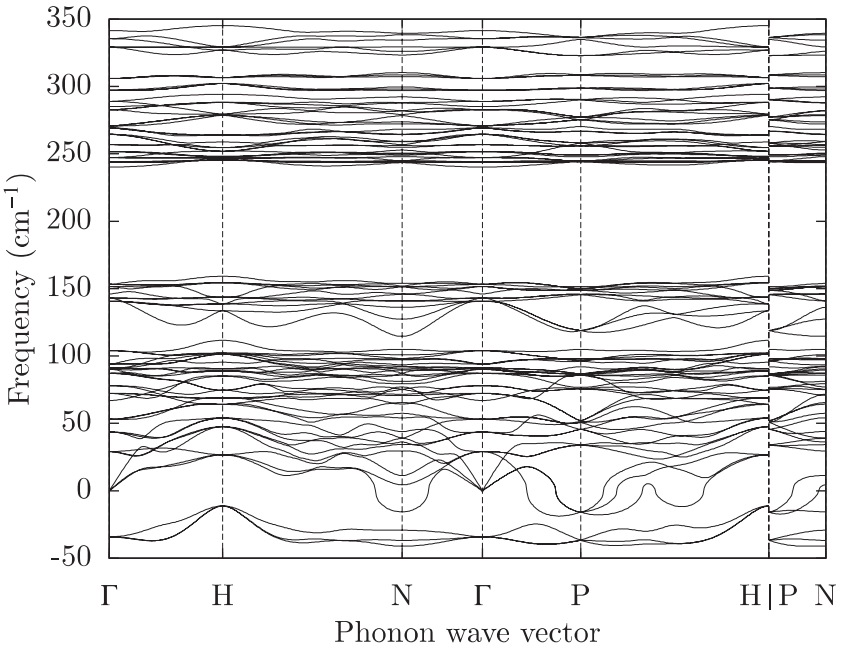

Figure 4. Calculated phonon dispersion of $Cu_{12}Sb_4S_{13}$ showing harmonically unstable vibrational modes involving out-of-plane vibrations of three-fold coordinated Cu atoms.

here, each Fe atom can provide an extra electron to fill holes in the valence band compared to each Zn atom, and explains why Fe substitution causes a larger increase in resistivity for the same x value. Our DFT calculations confirm this interpretation, showing that iron in $Cu_{11}FeSb_4S_{13}$ is indeed in the Fe^{3+} s^0d^5 configuration due to the formation of an exchange gap of approximately 3 eV between the Fe majority and minority spin states, which pushes the latter above the valence band maximum (see Supporting Information).

In order to understand the relationship between composition and the resulting zT values, we introduce the notion of the fraction (f) of hole states filled in the valence band upon substitution: $f = xN_e/2$, where N_e is the number of excess contributed electrons from each M ion. For example, for $x = 0.5$ Fe substitution ($N_e = 2$), the fraction is 0.5, while for $x = 0.5$ Zn substitution ($N_e = 1$), the fraction is 0.25. Figure 5b displays the relationship between filling fraction of holes and the measured zT values. For both substitutions, the maximum zT values are reached at 0.5 and zT begins to diminish for higher filling fraction. From this plot we see that zT values above 0.8 can be attained over a surprisingly large range of composition; high zT is extremely robust against impurity substitution on the copper site in $Cu_{12}Sb_4S_{13}$, with high values maintained up to a hole filling fraction of 0.8, even if the substitution is a mixture of more than one kind of atom. Since this range of substitution over which high zT is maintained exceeds significantly the range of composition of natural tetrahedrites, it is quite likely that natural mineral tetrahedrites can be used *directly* as thermoelectric materials.

To illustrate what one may achieve using natural mineral source material, we have obtained a natural tetrahedrite specimen from a mineral supplier.[25] The specimen was chosen at random from a selection of crystals denoted by gemological standards as tetrahedrite. A photograph of the specimen is shown in the Supporting Information. X-ray analysis indicated that the specimen indeed possessed the tetrahedrite crystal structure, but with a slight shift of peaks to higher angles. Under SEM observation with an energy-dispersive x-ray analysis microprobe, we found that this specimen was in fact a solid solution of tetrahedrite and tennantite. This is not surprising, since, as previously mentioned, almost all naturally occurring "tetrahedrite" minerals are of compositions along the tetrahedrite/tennantite solid solution. Further, we found that this specimen contained predominantly Fe substitution on the Cu site; the overall average composition was $Cu_{10.5}Fe_{1.5}As_{3.6}Sb_{0.4}S_{13}$. Thus, according to Figure 5b, we would not expect it to have optimized thermoelectric properties. The crystal was then powder processed in a manner identical to that used for our synthetic specimens and the thermoelectric properties measured. Indeed, we find high resistivity (Figure 2a), high Seebeck coefficient (Figure 2c), and low power factor. For this natural sample, the hole state filling fraction is near unity. Next, the natural mineral powder was mixed in a 1:1 weight ratio with our previously prepared synthetic powder of composition $Cu_{12}Sb_4S_{13}$, and this powder mixture was re-hot-pressed at 450 °C for 30 minutes. The resulting pellet was single phase tetrahedrite, with x-ray peaks approximately midway between those of the original natural mineral and the synthetic tetrahedrite specimen. This simple and very quick process allows for the "dilution and adjustment" of the Fe content in the natural specimen, and we estimate that the resulting pellet had a nominal composition of $Cu_{11.25}Fe_{0.75}As_{1.8}Sb_{2.2}S_{13}$. Indeed, we found that the resistivity of this "diluted" natural specimen (Figure 2a) was decreased by a factor of twenty and the power factor and figure of merit (Figure 5a) became comparable to that of the synthetic $Cu_{10.5}Zn_{1.5}Sb_4S_{13}$ and $Cu_{11.3}Fe_{0.7}Sb_4S_{13}$ samples.

While the natural mineral chosen and studied here did not have optimal composition for high figure of merit, there are very widespread deposits of natural tetrahedrites and tennantites with compositions in the range of high thermoelectric performance. Examples are the Zn-containing tetrahedrite/tennantite deposits in the Bruncu Sa Casa sector of the Furtei mine in Sardinia, Italy,[26] the Zn-rich ores in the Kuroko deposits in Japan,[27] and the Sb-rich tetrahedrite/tennantites in the Schwaz mines of North Tyrol, Austria.[28] It is highly likely that pellets of compacted powders of these natural minerals will display thermoelectric behavior equivalent to that demonstrated here in our synthetic specimens.

3. Conclusion

In conclusion, we have successfully synthesized single phase and high density Zn and Fe substituted $Cu_{12}Sb_4S_{13}$ of

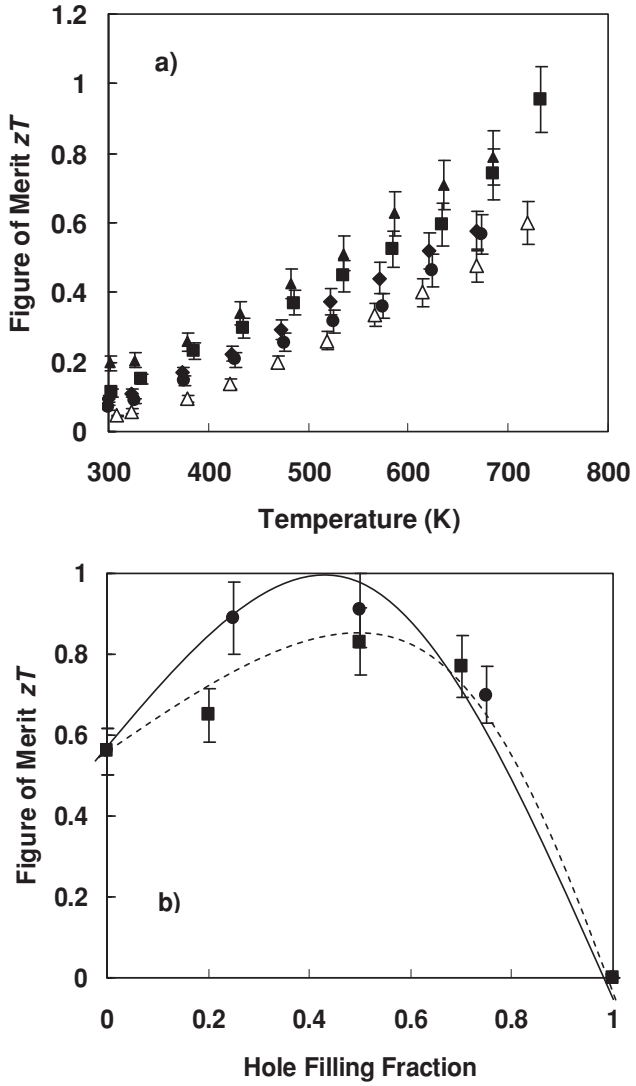

Figure 5. The thermoelectric figure of merit of tetrahedrite. a) dimensionless thermoelectric figure of merit zT as a function of temperature for tetrahedrite $Cu_{12-x}Zn_xSb_4S_{13}$. zT rises with increasing Zn content up to x = 1.0, but stays large even for x = 1.5. Because the lattice thermal conductivity of these compounds is so small, the electronic thermal conductivity plays a special role in controlling their thermoelectric properties. With increasing Zn content, the resistivity rises, causing the power factor to decrease, but this is more than made up for by a decrease in electronic thermal conductivity. By slight adjustment of the composition of the pellet synthesized from natural source tetrahedrite, high zT is attained. Sample designation as in Figure 2a). b) Figure of merit versus fraction of hole states filled in the valence band for $Cu_{12-x}M_xSb_4S_{13}$ (M = Zn, Fe). zT reaches a maximum at smaller concentrations for Fe due to its variable valence state.

composition range covering that of naturally occurring tetrahedrite. The intrinsic low lattice thermal conductivities give birth to high zT values comparable to state of art thermoelectric materials in the range of 600–700 K. A thermoelectric figure of merit above 0.8 can be maintained over a large range of substitution level, and is related to the filling of hole states in the valence band. Additionally, we show that a comparable value of zT can be achieved in a randomly chosen natural tetrahedrite mineral specimen, with composition adjusted by a simple and quick process. Investigations of the thermoelectric properties of minerals is not a new idea; in fact, Seebeck's original work[29] was largely based on natural materials, and a detailed study was undertaken by Telkes[30] in 1953. Here, we bring to bear powerful modern tools, including electronic band structure and lattice dynamics calculations, to shed new light on this old problem. We believe that our work creates a new paradigm for thermoelectric materials. In a traditional process, minerals are mined and pure elements extracted from them with great effort and expense; these purified elements are then carefully recombined into new compounds at additional great effort and expense. In the new process outlined here, minerals can be mined and used *directly* or with very little additional processing to achieve high thermoelectric performance from earth abundant materials with little effort and low cost.

4. Experimental and Theoretical Section

Sample Preparation: $Cu_{12}Sb_4S_{13}$ samples were synthesized by direct solid state reaction of the starting elements- Cu(99.99%, Alfa-Aesar), Sb(99.9999%, Alfa-Aesar), and S, Zn,Fe (99.999%, Alfa-Aesar). These raw materials were loaded in stoichiometric ratios into quartz ampoules that were evacuated to $<10^{-5}$ Torr. The loaded ampoules were then placed into a vertical furnace and heated at 0.3 °C min^{-1} to 650 °C and held at that temperature for 12 hours. Subsequently, they were slowly cooled to room temperature at the rate of 0.4 °C min^{-1}. The resulting reacted material was placed into a stainless steel vial and ball milled for five minutes in a SPEX sample preparation machine. These ball-milled powders were then cold pressed into a pellet and re-ampouled under vacuum for annealing for two weeks at 450 °C. The final product after annealing was ball milled for 30 min into fine powders and hot-pressed under argon atmosphere at 80 MPa pressure and 430 °C for 30 min. We also synthesized specimens using powder obtained from a natural tetrahedrite crystal. This crystal was powdered and processed, both directly and after mixing in a 1:1 weight ratio with synthetic $Cu_{12}Sb_4S_{13}$ powder, using the same procedure as described above. All the hot pressed samples used in this study were greater than 98% theoretical density, as measured using the Archimedes method.

Characterization: X-ray diffraction analysis was performed by using a Rigaku Miniflex II bench-top X-ray diffractometer (Cu K_α radiation), and the results analyzed using a Jade software package. High temperature (373 K – 673 K) Seebeck coefficient and electrical resistivity were measured in an Ulvac ZEM-3 system under argon. The thermal diffusivity (D) and heat capacity (C_p) from 373 K to 673 K were measured using the laser flash method (Netzsch, LFA 457) and differential scanning calorimetry (Netzsch, DSC200F3) respectively. The data were also confirmed independently in a second laboratory using an Anter Flashline 5000 thermal diffusivity apparatus and a Netzsch 404 C Pegasus calorimeter. The samples used for these measurements were from adjacent sections of the same pellets as those used for high temperature resistivity and Seebeck coefficient The high temperature thermal conductivity was calculated using $\kappa = D*C_p*$density. We estimate an error of approximately 3% each in resistivity and Seebeck coefficient, and 8% in thermal conductivity, yielding a quadrature error in power factor of approximately 5% and in zT of approximately 10%. These values are reflected by the error bars in the plots.

Theory: Density-functional theory (DFT) calculations were performed with the projector-augmented wave (PAW) method as implemented in the highly efficient Vienna *Ab Initio* Simulation Package (VASP).[31] Our self-consistent calculations used regular Monkhorst-Pack k-point meshes (where k is the electron wavevector) of 10 ×10 × 10 and a plane wave cutoff energy of 450 eV. The Perdew-Becke-Ernzerhof (PBE) exchange-correlation (xc) functional[32] was used to obtain the band structure

shown in Figure 2. To test the validity of the PBE functional, separate calculations were performed using the LDA+*U* method[33] with *U* values of 4 and 8 eV, as well as with the Heyd-Scuseria-Ernzerhof (HSE06) range-separated hybrid exchange functional.[34] The band structure near the Fermi level was found to be qualitatively unchanged w.r.t. the choice of the xc functional. Phonon dispersion curves were calculated using an in-house DFT linear response code. Optimized norm-conserving pseudopotentials were generated for Cu $3d^{10}4s^1$, Sb $5s^25p^3$, and S $3s^23p^4$ valence configurations. Electronic wave functions were expanded in plane wave basis with a 680 Ry cutoff energy and the Brillouin zone was sampled on a regular $8 \times 8 \times 8$ k-point mesh. Dynamical matrices were calculated on a regular $2 \times 2 \times 2$ k-point grid and interatomic force constants were obtained via inverse Fourier transform; these force constants were then used to interpolate phonon dispersion throughout the Brillouin zone. Phonon mode Grüneisen parameters were obtained by taking finite differences between phonon frequencies calculated at two lattice parameters separated by 2%.

Supporting Information

Supporting Information is available from the Wiley Online Library or from the author.

Acknowledgements

This collaborative work was supported at MSU and UCLA as part of the Center for Revolutionary Materials for Solid State Energy Conversion, an Energy Frontier Research Center funded by the U.S. Department of Energy, Office of Science, Office of Basic Energy Sciences under Award Number DE-SC0001054, and at UM as part of the Center for Solar and Thermal Energy Conversion, an Energy Frontier Research Center funded by the U.S. Department of Energy, Office of Science, Office of Basic Energy Sciences under Award No. DE-SC0000957. Calculations were done using resources of the National Energy Research Scientific Computing Center (NERSC), which is supported by the Office of Science of the U.S. Department of Energy under Contract No. DE-AC02-05CH11231. We acknowledge illuminating discussions with Dr. Christopher J. Stefano on the geology of tetrahedrites.

Received: August 17, 2012
Published online: October 18, 2012

[1] R. Venkatasubramanian, E. Siivola, T. Colpitts, B. O'Quinn, *Nature* **2001**, *413*, 597.
[2] B. C. Sales, D. Mandrus, R. L. Williams, *Science* **1996**, *272*, 1325.
[3] H. Li, X. Tang, Q. Zhang, C. Uher, *Appl. Phys. Lett.* **2009**, *94*, 102114.
[4] G. Rogl, Z. Aabdin, E. Schafler, J. Horky, D. Setman, M. Zehetbauer, M. Kriegisch, O. Eibl, A. Grytsiv, E. Bauer, M. Reinecker, W. Schranz, P. Rogl, *J. Alloys Compd.* **2012**, *537*, 183.
[5] X. Shi, J. Yang, J. R. Salvador, M. Chi, J. Y. Cho, H. Wang, S. Bai, J. Yang, W. Zhang, L. Chen, *Journal of the American Chemical Society* **2011**, *133*, 7837.
[6] C. Uher, in *Semiconductors and Semimetals*, Vol. *69* (ed. T. M. Tritt), Academic Press, San Diego, **2001**, Ch. 5.
[7] B. Poudel, Q. Hao, Y. Ma, Y. Lan, A. Minnich, B. Yu, X. Yan, D. Wang, A. Muto, D. Vashaee, X. Chen, J. Liu, M. S. Dresselhaus, G. Chen, Z. Ren, *Science* **2008**, *320*, 634.
[8] K. Biswas, J. He, Q. Zhang, G. Y. Wang, C. Uher, V. Dravid, M. G. Kanatzidis, *Nat. Chem.* **2011**, *3*, 160.
[9] S. Girard, J. He, C.-P Li, S. Moses, G. Y. Wang, C. Uher, V. Dravid, M. G. Kanatzidis, *Nano Lett.* **2010**, *10*, 2825.
[10] R. J. Mehta, Z Yanliang, C. Karthik, B. Singh, R. W. Siegel, T. Borca-Tasciuc, G. Ramanath, *Nat. Mater.* **2012**, *11*, 233.
[11] G. A. Slack, in *CRC Handbook of Thermoelectrics* (ed. D. M. Rowe), CRC Press, Boca Raton, **1995**, Ch. 34.
[12] G. A. Slack, in *Solid State Physics* (ed. H. Ehrenreich, F. Weitz, and D. Turnbull) Academic Press, New York **1979**, p. 1.
[13] D. G. Cahill, R. O. Pohl, *Phys. Rev. B* **1987**, *35*, 4067.
[14] G. S. Nolas, G. A. Slack, *Am. Sci.* **2001**, *89*, 136.
[15] D. T. Morelli, V. Jovovic, J. P. Heremans, *Phys. Rev. Lett.* **2008**, *101*, 035901.
[16] E. J. Skoug, D. T. Morelli, *Phys. Rev. Lett.* **2011**, *107*, 235901.
[17] R. Berman, *Thermal Conduction in Solids*, Oxford, London **1976**.
[18] Y. Zhang, E. J. Skoug, J. Cain, V. Ozoliņs, D. T. Morelli, C. Wolverton, *Phys. Rev. B* **2012**, *85*, 054306.
[19] D. T. Morelli, J. P. Heremans, G. A. Slack, *Phys. Rev. B* **2002**, *66*, 195304.
[20] B. J. Wuensch, *Zeitschrift Kristall.* **1964**, *119*, 437.
[21] A. Pfitzner, M. Evain, V. Petricek, *Acta Crystall.* **1997**, *B53*, 337.
[22] J. W. Miller, J. R. Craig, *Am. Mineral.* **1983**, *68*, 227.
[23] K. Suekuni, K. Tsuruta, T. Ariga, M. Koyano, *Appl. Phys. Express* **2012**, *5*, 051201.
[24] E. Mackovicky, K. Forcher, W. Lottermoser, G. Amthauer, *Mineral. Petrol.* **1990**, *43*, 73.
[25] Stefano Fine Minerals, Inc., Ann Arbor, Michigan USA.
[26] S. Fadda, M. Fiori, S. M. Grillo, *Geochem., Mineral., Petrol.* **2005**, *43*, 79.
[27] S. Kitazono, H. Ueno, *Resource Geol.* **2003**, *53*, 143.
[28] T. Arlt, L. W. Diamond, *Mineral. Mag.* **1998**, *62*, 801.
[29] T. J. Seebeck, *Abh. Akad. Wiss.* Berlin **1822**, *1820–21*, 289.
[30] M. Telkes, *Amer. Mineral.* **1950**, *35*, 536.
[31] a) J. Kresse, G. Hafner, *Phys. Rev. B* **1993**, *47*, 558; b) J. Kresse, D. Joubert, *Phys. Rev. B* **1999**, *59*, 1758.
[32] J. P. Perdew, K. Burke, M. Ernzerhof, *Phys. Rev. Lett.* **1996**, *77*, 3865.
[33] A. I. Liechtenstein, V. I. Anisimov, J. Zaanen, *Phys. Rev. B* **1995**, *52*, R5467.
[34] J. Heyd, G. E. Scuseria, M. Ernzerhof, *J. Chem. Phys.* **2006**, *124*, 219906.